Galactic and Extragalactic Analysis of the Astrophysical Muon Neutrino Flux with 12.3 years of IceCube Track Data

N.B. When citing this work, cite the original published paper.

(article starts on next page)

Galactic and Extragalactic Analysis of the Astrophysical Muon Neutrino Flux with 12.3 years of IceCube Track Data

The IceCube Collaboration

(a complete list of authors can be found at the end of the proceedings)

E-mail: philipp.fuerst@icecube.wisc.edu

The Ice Cube Neutrino Observatory has been measuring an isotropic astrophysical neutrino flux in multiple detection channels for almost a decade. Galactic diffuse emission, which arises from the interactions between cosmic rays and the interstellar medium, is an expected signal in IceCube. The superposition of an extragalactic flux and a galactic flux results in directional structure and variations in the spectrum. In this work, we use 12.3 years of high-purity muon-neutrino induced muon track data to perform a dedicated search for this galactic emission, combined with a spectral measurement of the isotropic astrophysical neutrino flux. To distinguish a galactic component from the dominant atmospheric and isotropic astrophysical components, the precise directional information available for muon tracks is fully utilized in a three-dimensional forward folding likelihood fit. We test a state-of-the-art model prediction of galactic diffuse emission based on recent cosmic ray data (CRINGE). We fit this prediction as a template scaled by a factor Ψ_{CRINGE}, and find $2.9 \pm 1.1 \times \Psi_{\text{CRINGE}}$ with a significance of 2.7σ in an energy range between $400\,\text{GeV}$ and $60\,\text{TeV}$ in the Northern Sky.

Corresponding authors: Philipp Fürst[1]

[1]*RWTH Aachen University*

ICRC2023
38th International Cosmic Ray Conference
The Astroparticle Physics Conference

1. Introduction

Galactic diffuse neutrino emission from hadronic interactions between cosmic rays and the interstellar medium of our galaxy can serve as a direct tracer for cosmic rays and is an expected signal for IceCube. Neutrino emission from the galactic plane has very recently been observed for the first time with high significance by IceCube [1, 2], emerging as a non-isotropic, subdominant component from the long-observed diffuse astrophysical neutrino flux.

Here, we present an update to one of the analyses investigating this isotropic diffuse flux [3]. We use 12.3 years of track data from the northern hemisphere and extend the analysis variables of reconstructed energy proxy and zenith angle by a third dimension by including right ascension information. This enables a combined measurement of both the isotropic flux, identified by its high-energy signature where it dominates over atmospheric backgrounds, and a galactic signal, identified by its unique spatial structure on the sky. Atmospheric backgrounds are completely isotropized in right ascension due to the rotation of the Earth. The baseline signal hypothesis is formulated as an isotropic single powerlaw and an additional component from galactic diffuse emission [4], see Sec. 3. Additionally, different model calculations for galactic diffuse emission are tested [5–7], providing hints about the structure of this galactic emission.

2. IceCube Detector and Selection of Data Sample

The IceCube Neutrino Observatory was built to detect astrophysical neutrinos, which it discovered in 2013 [8]. It has been measuring their spectrum in multiple detection channels since, with the most recent results presented at this conference [9–11].

Charged secondaries produced by deep inelastic scattering (*DIS*) of neutrinos and matter produce a detectable signature of Cherenkov light. IceCube instruments about $1\,\mathrm{km}^3$ of natural ice at the South Pole to detect this light, embedding 5160 digital optical modules (DOMs) in depths between $1.5\,\mathrm{km}$ and $2.5\,\mathrm{km}$ in the ice. The DOMs are mounted on a total of 86 vertical cables (strings) [12]. Possible secondaries of *DIS* include high-energy muons, which can travel up to several kilometers in ice, creating a track-like signature in the detector.

This analysis is based on a selection of such track-like events. It utilizes boosted decision trees trained to distinguish high-quality tracks from spherical cascade topologies (which occur for example from ν_e interactions) and a background of tracks induced by atmospheric muons, which dominate the flux from the Southern Sky. A zenith cut of $\Theta_{\mathrm{zenith}} > 85°$ is applied, so only events which travelled through the Earth or substantial amounts of Antarctic ice and rock are accepted. This effectively shields the sample from muons created in the atmosphere by cosmic ray interactions, resulting in a neutrino purity $> 99.8\%$, at the cost of removing the hemisphere including the galactic center. The analysis region includes the section of the galactic plane with longitudes $< -141°$ and $> 27°$.

This event selection has been used for measurements of the astrophysical neutrino flux [3, 13], including a test for a galactic plane contribution [14]. Here, we extend the data sample to a total of 12.3 years of data collected between June, 2010 and January 2023, resulting in a 45% increase in event numbers compared to the previous analysis [3]. Data-taking seasons when the detector was running in partially-completed configurations such as IC59 (with 59 strings deployed) are excluded

in favor of a unified detector simulation. The IC79 season has been shown to be sufficiently similar to the full IC86 configuration when weighted with a detection efficiency of 94% [3] and is included. This yields a total of 982,279 up-going, track-like events with a median angular resolution of $< 1°$ above 1 TeV and $< 0.25°$ above 1 PeV.

3. Analysis Method

The analysis is based on a forward-folding, three dimensional binned likelihood fit. The analysis dimensions are a muon energy proxy, *truncated energy* [15], and two angles of reconstructed event direction. The direction is calculated using the *MPE* algorithm [16] in coordinates of IceCube zenith Θ and right ascension RA. Data events are sorted into their respective bins (50 in energy proxy between 100 GeV and 10 PeV, 33 in $\cos\Theta$ and 180 in RA), yielding n_{bin} data events per bin, and are compared to the expectation μ_{bin} calculated from simulated events. The expectation is a function of signal $\vec{\Theta}$ and nuisance parameters $\vec{\xi}$, and the maximum of the Poisson-likelihood $\mathcal{L}$ given the data D yields the best-fit signal parameters:

$$\mathcal{L}(D|\vec{\Theta},\vec{\xi}) = \sum_{\text{bin}}^{N_{\text{bins}}} p_{\text{Poisson}}(n_{\text{bin}}, \mu_{\text{bin}}(\vec{\Theta},\vec{\xi})). \tag{1}$$

The nuisance parameters $\vec{\xi}$ consist of two groups, the first one describes overall detector uncertainties and the second the background fluxes. The parameterization closely follows a previous analysis of this data sample using 9.5 years of data [3].

Detector uncertainties arise from the overall light collection efficiency of the DOMs and absorption and scattering properties of the glacial ice. Additionally, the effects of impurities and bubbles produced by the re-freezing of water in the boreholes are included. These are modeled as an acceptance function depending on incident angle for the DOMs. Compared to [3], a second parameter describing this angular acceptance function has been added, affecting the possible zenith distribution of the fitted fluxes. This results in a total of five detector uncertainty parameters.

Across the sky, and for energies below ≈ 200 TeV, the dominating background arises from atmospheric neutrinos. Conventional and prompt atmospheric fluxes are updated compared to [3] using the *MCEq*-package [17], version 1.2.1. The cosmic ray primary flux is modeled with the *H4a* model [18], and for interactions in the atmosphere the hadronic interaction model *Sibyll2.3c* is employed [19]. Uncertainty of the cosmic ray primary flux is covered by a combination of a free global spectral index shift and a parameter interpolating linearly between the *H4a* and *GST* [20] models. The uncertainties of pion and kaon production in cosmic ray air showers are modeled following the *Barr* formulation [21]. A sub-dominant component from atmospheric muons which are mis-reconstructed as up-going is simulated using the *CORSIKA* package [22] and has a free normalization scale in the fit. In total, this formulation yields a number of $n_{\vec{\xi}} = 14$ nuisance parameters.

Two signal flux components are considered: an isotropic, astrophysical signal and a non-isotropic signal from the galactic plane. The isotropic signal is modeled as a single powerlaw (Eq. 2), and it is the only astrophysical component included in the baseline hypothesis H_0 (no galactic contribution). The galactic contribution is modeled following the CRINGE prediction for diffuse
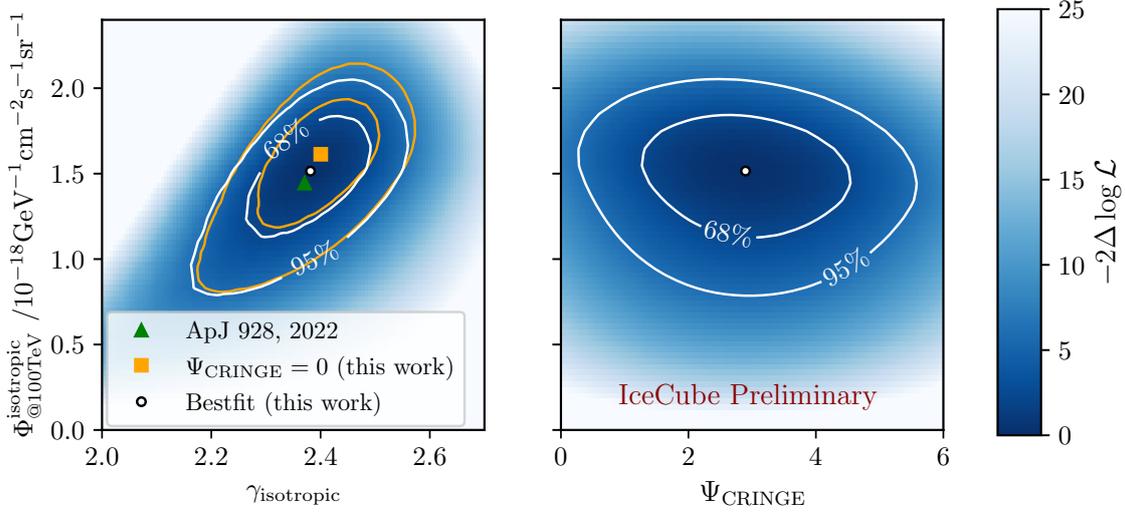
Figure 1: Likelihood landscape as a function of the signal parameters $\Phi_{\text{isotropic}}$ (y-axis for both figures), $\gamma_{\text{isotropic}}$, and Ψ_{CRINGE}. The green triangle marks the result from [3], which did not consider a galactic contribution. The updated background calculations and removal of the IC59 data account for the observed shift towards the orange square, which is the 12.3 year fit without a galactic plane contribution. The best-fit normalization including a galactic component (white point) is 6.5% lower.

emission from [4]. It is based on a fit to cosmic-ray data from multiple experiments and explores uncertainties arising from other required ingredients such as gas maps and cross sections. We preserve the complex spectral and spatial features of the prediction, which vary across the sky, but allow an overall free normalization scale Ψ_{CRINGE}. This yields $n_{\vec{\Theta}} = 3$ signal parameters.

4. Results

The null-hypothesis H_0 of no galactic contribution is excluded with a significance of 2.7σ, and we fit a galactic contribution of $\Psi_{\text{CRINGE}} = 2.9 \pm 1.1$ for our baseline model, which was chosen a priori. This template normalization corresponds to $1100\pm_{410}^{420}$ events, or 1.1% of the total events. We fit an isotropic astrophysical component of $\phi_{\text{isotropic}} = 1.51\pm_{0.23}^{0.22}$ and $\gamma = 2.38\pm_{0.08}^{0.08}$ when described as a single powerlaw:

$$\Phi_{\text{isotropic}}^{\nu_\mu + \vec{\nu}_\mu} = \phi_{\text{isotropic}} \times \left(\frac{E}{100\,\text{TeV}}\right)^{-\gamma} \times 10^{-18}\text{GeV}^{-1}\text{cm}^{-2}\text{s}^{-1}\text{sr}^{-1}. \tag{2}$$

If the galactic component is neglected, we find a spectral index of $\gamma = 2.40$ and the normalization increases by 6.5%, see Fig. 1. The energy-projection of the analysis histogram with best-fit spectra is shown in Fig. 2.

4.1 Model differentiation

As alternatives to our baseline model hypothesis [4], other calculations for galactic diffuse neutrino emission are tested: the Fermi-π^0 [5] and KRA$_\gamma$ models [6], which are based on Fermi-LAT data. The Fermi-π^0-model extrapolates the observed spectral index of 2.7 as a single powerlaw.
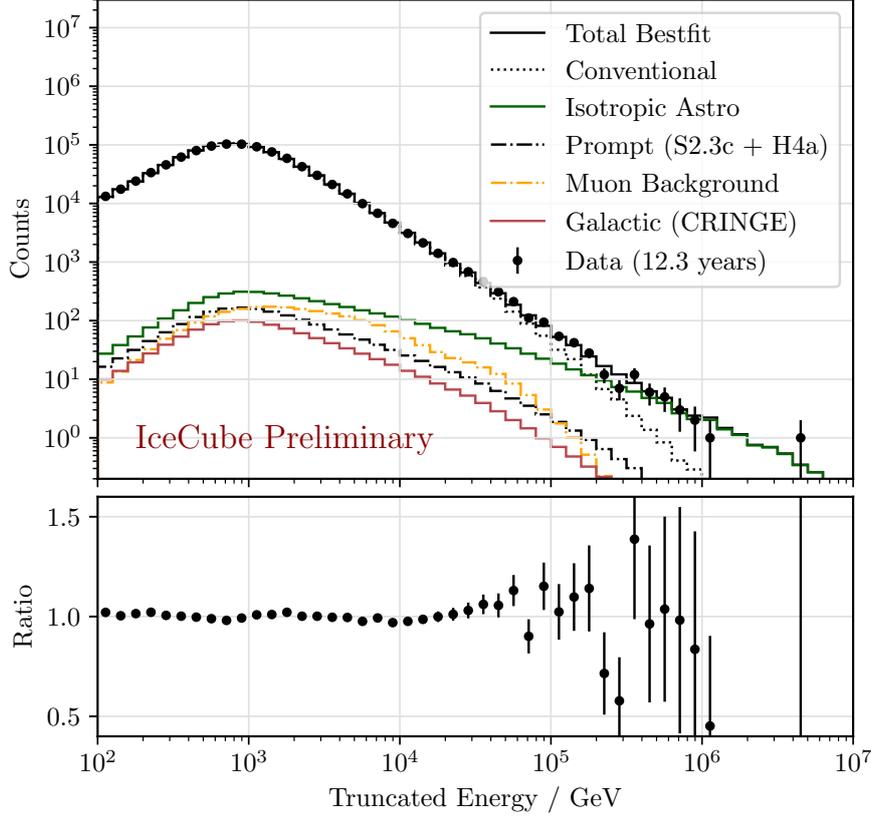
Figure 2: Data and bestfit results as function of the muon energy proxy. The dominating conventional atmospheric flux (black dotted line) is very similar to the total sum except for the highest energies, where the isotropic astrophysical signal (dark green) starts to dominate. The best-fit prefers no prompt atmospheric flux contribution, shown here is the prediction modeled with *MCEq*, see Section 3 (black dashdotted). The muon background (orange) arises from mis-modeled atmospheric events which were misreconstructed as up-going. The best-fit galactic flux (dark red) contributes about 1.1% to the total observed rate.

The KRA$_\gamma$ formulation assumes a radial dependence for cosmic ray diffusion, leading to a spectral hardening towards the galactic center. It contains a variable cutoff at 5(50) PeV in the galactic cosmic ray spectrum, yielding the KRA$_\gamma^{5(50)}$ models. Finally, we test for two analytic models following Fang&Murase [7], which assume a factorization of gas and cosmic ray density from the line of sight integral. The galactic disk is then homogeneously filled assuming the radial distribution to be either constant or to follow the distribution of supernova-remnants. For the spectrum we chose a single powerlaw analogously to Fermi-π^0 with a spectral index of $\gamma = 2.7$. These models (FM-const and FM-SNR) result in predictions following the geometry of the galactic disk and are independent of any gas structure.

We test all these alternative hypotheses against our baseline model by measuring the test-statistic $x = \log \mathcal{L}(H_{\text{alternative}}) - \log \mathcal{L}(H_{\text{Cringe}})$ for all models. To determine the significance, the TS-distribution is obtained from pseudo-experiments, which are drawn assuming one of the two hypotheses to be true, resulting in two distributions: $TS|\text{Cringe} = \log \mathcal{L}(H_{\text{alternative}}|\text{Cringe}) - \log \mathcal{L}(H_{\text{Cringe}}|\text{Cringe})$ and $TS|\text{alternative}$. An example of this procedure is shown in Fig. 3. All
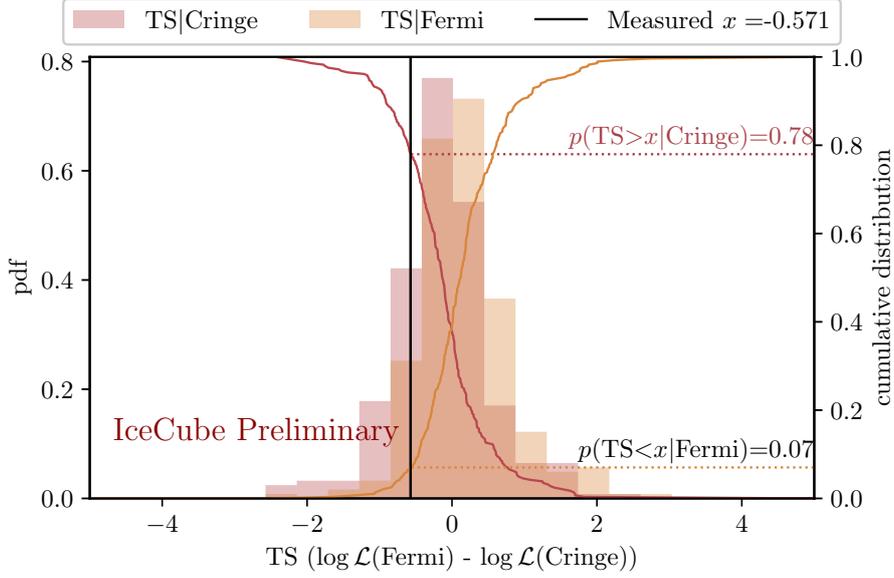
Figure 3: Example for a model differentiation test with the Fermi-π^0 model. Each TS distribution is calculated from 600 pseudoexperiments. The quantiles are integrated from the left (right) for the alternative (baseline) model.

Model	fitted Ψ_{model}	x	$p(TS < x \vert \text{Model})$	$p(TS > x \vert \text{Cringe})$
Fermi-π^0	$4.7 \pm^{+2}_{-2}$	-0.571	0.07	0.78
KRA$^{50}_{\gamma}$	$0.7 \pm^{+0.4}_{-0.4}$	-1.12	0.032	0.545
KRA$^{5}_{\gamma}$	$1 \pm^{+0.5}_{-0.5}$	-0.85	0.054	0.63
FM-SNR	$1.6 \pm^{+0.8}_{-0.8}$	-2.695	0.023	0.854
FM-const	$0.8 \pm^{+0.6}_{-0.6}$	-1.304	0.002	0.896

Table 1: Model differentiation tests. All models fit a nonzero galactic flux and measure $x < 0$ (baseline hypothesis preferred). The significance of this preference (p-value) is calculated here only conditionally, assuming either the baseline or the alternative model to be true.

resulting p-values from the tests are shown in Tab. 1. While we measure $x < 0$ for all tests, it is currently not possible to establish a preferred model.

5. Conclusion

We present an updated measurement of the diffuse astrophysical neutrino flux using 12.3 years of IceCube track data, measuring an isotropic component described as a single powerlaw with the parameters $\phi_{\text{isotropic}} = 1.51\pm^{0.22}_{0.23}$ and $\gamma = 2.38\pm^{0.08}_{0.08}$. We observe a preference for a galactic contribution in the Northern Sky at the 2.7σ level. Removing this component increases the measured isotropical flux normalization by about 6.5%. This result is consistent with the first observation of neutrino emission from the galactic plane, which is based on a dedicated selection of IceCube cascade events, and which fitted a very similar overall model normalization for the Fermi-π^0 model with a significance of 4.7σ [1, 2]. It is also consistent with a test for a galactic contribution using
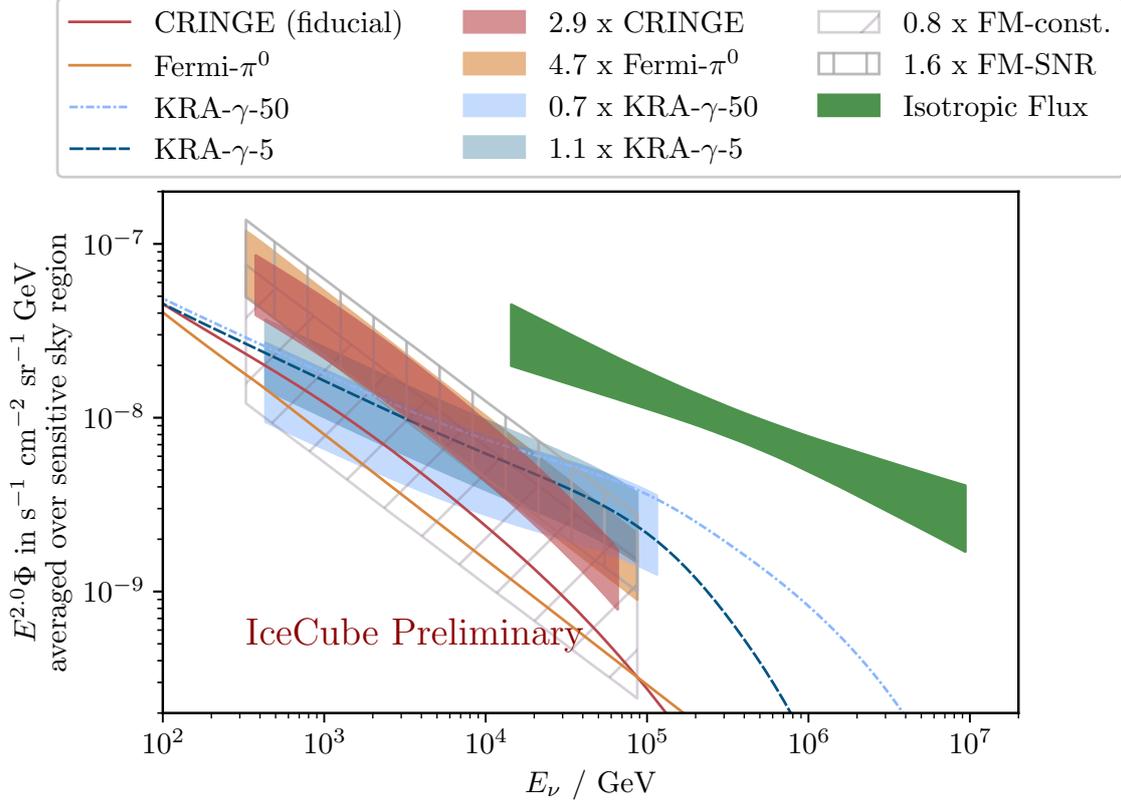
Figure 4: Unfolded Spectra of the two fitted neutrino flux contributions. The shown 68% error bands are constructed by variation of the signal parameters inside the likelihood space. Model predictions for galactic diffuse emission which are based on gas maps are shown as lines.

starting track events [10]. Although the difference is not statistically significant, it is interesting to note that the fitted model scales for the KRA-models are a factor ≈ 2 larger in this Northern Sky measurement than in the all-sky cascade analysis.

For the Northern Sky, these measurements paint a consistent first picture of a neutrino flux from the galactic plane which is moderately stronger than the most recent model predictions for a diffuse-emission only scenario suggest (not considering contributions from unresolved sources) [4]. However, obtaining any information on the spectral and spatial structure of this signal will require significantly more data, which could for example be achieved following ideas as outlined in [23] and [9] by moving towards global analyses of IceCube data.

References

[1] **IceCube** Collaboration, M. Aartsen *et al. Science* **380** no. 6652, (2023) 1338–1343.

[2] **IceCube** Collaboration *PoS* **ICRC2023** (these proceedings) 1108.

[3] **IceCube** Collaboration, R. Abbasi *et al. Astrophysical Journal* **928** (Mar., 2022) .

[4] G. Schwefer, P. Mertsch, and C. Wiebusch *The Astrophysical Journal* **949** (05, 2023) 16.

[5] **Fermi LAT** Collaboration, M. Ackermann *et al. The Astrophysical Journal* **750** no. 1, (Apr, 2012) 3.

[6] D. Gaggero, D. Grasso, A. Marinelli, A. Urbano, and M. Valli *The Astrophysical Journal Letters* **815** no. 2, (Dec, 2015) L25.

[7] K. Fang and K. Murase *The Astrophysical Journal* **919** no. 2, (Sep, 2021) 93.

[8] **IceCube** Collaboration, M. Aartsen *et al. Science* **342** no. 6161, (2013) 1242856.

[9] **IceCube** Collaboration *PoS* **ICRC2023** (these proceedings) 1064.

[10] **IceCube** Collaboration *PoS* **ICRC2023** (these proceedings) 1008.

[11] **IceCube** Collaboration *PoS* **ICRC2023** (these proceedings) 1007.

[12] **IceCube** Collaboration, M. Aartsen *et al. Journal of Instrumentation* **12** no. 03, (Mar, 2017) P03012.

[13] **IceCube** Collaboration, M. Aartsen *et al. The Astrophysical Journal* **833** no. 1, (Dec., 2016) 3.

[14] C. Haack, *Observation of high-energy neutrinos from the galaxy and beyond*. Dissertation, RWTH Aachen University, 2020.

[15] **IceCube** Collaboration, R. Abbasi *et al. Nuclear Instruments and Methods in Physics Research Section A* **703** (Mar., 2013) 190–198.

[16] **IceCube** Collaboration, J. Ahrens *et al. Nuclear Instruments and Methods in Physics Research Section A* **524** no. 1, (May, 2004) 169–194.

[17] A. Fedynitch, R. Engel, T. K. Gaisser, F. Riehn, and T. Stanev *EPJ Web Conf.* **99** (2015) 08001.

[18] T. K. Gaisser *Astroparticle Physics* **35** no. 12, (Jul, 2012) 801–806.

[19] A. Fedynitch, F. Riehn, R. Engel, T. K. Gaisser, and T. Stanev *Phys. Rev. D* **100** no. 10, (Nov., 2019) 103018.

[20] T. K. Gaisser, T. Stanev, and S. Tilav *Frontiers of Physics* (Mar., 2013) .

[21] G. D. Barr, S. Robbins, T. K. Gaisser, and T. Stanev *Phys. Rev. D* **74** no. 9, (Nov., 2006) 094009.

[22] D. Heck, J. Knapp, J. Capdevielle, *et al. Tech. Rep. FZKA* **6019** (1998) .

[23] **IceCube** Collaboration *PoS* **ICRC2023** (these proceedings) 1010.

Full Author List: IceCube Collaboration

R. Abbasi[17], M. Ackermann[63], J. Adams[18], S. K. Agarwalla[40, 64], J. A. Aguilar[12], M. Ahlers[22], J.M. Alameddine[23], N. M. Amin[44], K. Andeen[42], G. Anton[26], C. Argüelles[14], Y. Ashida[53], S. Athanasiadou[63], S. N. Axani[44], X. Bai[50], A. Balagopal V.[40], M. Baricevic[40], S. W. Barwick[30], V. Basu[40], R. Bay[8], J. J. Beatty[20, 21], J. Becker Tjus[11, 65], J. Beise[61], C. Bellenghi[27], C. Benning[1], S. BenZvi[52], D. Berley[19], E. Bernardini[48], D. Z. Besson[36], E. Blaufuss[19], S. Blot[63], F. Bontempo[31], J. Y. Book[14], C. Boscolo Meneguolo[48], S. Böser[41], O. Botner[61], J. Böttcher[1], E. Bourbeau[22], J. Braun[40], B. Brinson[6], J. Brostean-Kaiser[63], R. T. Burley[2], R. S. Busse[43], D. Butterfield[40], M. A. Campana[49], K. Carloni[14], E. G. Carnie-Bronca[2], S. Chattopadhyay[40, 64], N. Chau[12], C. Chen[6], Z. Chen[55], D. Chirkin[40], S. Choi[56], B. A. Clark[19], L. Classen[43], A. Coleman[61], G. H. Collin[15], A. Connolly[20, 21], J. M. Conrad[15], P. Coppin[13], P. Correa[13], D. F. Cowen[59, 60], P. Dave[6], C. De Clercq[13], J. J. DeLaunay[58], D. Delgado[14], S. Deng[1], K. Deoskar[54], A. Desai[40], P. Desiati[40], K. D. de Vries[13], G. de Wasseige[37], T. DeYoung[24], A. Diaz[15], J. C. Díaz-Vélez[40], M. Dittmer[43], A. Domi[26], H. Dujmovic[40], M. A. DuVernois[40], T. Ehrhardt[41], P. Eller[27], E. Ellinger[62], S. El Mentawi[1], D. Elsässer[23], R. Engel[31, 32], H. Erpenbeck[40], J. Evans[19], P. A. Evenson[44], K. L. Fan[19], K. Fang[40], K. Farrag[16], A. R. Fazely[7], A. Fedynitch[57], N. Feigl[10], S. Fiedlschuster[26], C. Finley[54], L. Fischer[63], D. Fox[59], A. Franckowiak[11], A. Fritz[41], P. Fürst[1], J. Gallagher[39], E. Ganster[1], A. Garcia[14], L. Gerhardt[9], A. Ghadimi[58], C. Glaser[61], T. Glauch[27], T. Glüsenkamp[26, 61], N. Goehlke[32], J. G. Gonzalez[44], S. Goswami[58], D. Grant[24], S. J. Gray[19], O. Gries[1], S. Griffin[40], S. Griswold[52], K. M. Groth[22], C. Günther[1], P. Gutjahr[23], C. Haack[26], A. Hallgren[61], R. Halliday[24], L. Halve[1], F. Halzen[40], H. Hamdaoui[55], M. Ha Minh[27], K. Hanson[40], J. Hardin[15], A. A. Harnisch[24], P. Hatch[33], A. Haungs[31], K. Helbing[62], J. Hellrung[11], F. Henningsen[27], L. Heuermann[1], N. Heyer[61], S. Hickford[62], A. Hidvegi[54], C. Hill[16], G. C. Hill[2], K. D. Hoffman[19], S. Hori[40], K. Hoshina[40, 66], W. Hou[31], T. Huber[31], K. Hultqvist[54], M. Hünnefeld[23], R. Hussain[40], K. Hymon[23], S. In[56], A. Ishihara[16], M. Jacquart[40], O. Janik[1], M. Jansson[54], G. S. Japaridze[5], M. Jeong[56], M. Jin[14], B. J. P. Jones[4], D. Kang[31], W. Kang[56], X. Kang[49], A. Kappes[43], D. Kappesser[41], L. Kardum[23], T. Karg[63], M. Karl[27], A. Karle[40], U. Katz[26], M. Kauer[40], J. L. Kelley[40], A. Khatee Zathul[40], A. Kheirandish[34, 35], J. Kiryluk[55], S. R. Klein[8, 9], A. Kochocki[24], R. Koirala[44], H. Kolanoski[10], T. Kontrimas[27], L. Köpke[41], C. Kopper[26], D. J. Koskinen[22], P. Koundal[31], M. Kovacevich[49], M. Kowalski[10, 63], T. Kozynets[22], J. Krishnamoorthi[40, 64], K. Kruiswijk[37], E. Krupczak[24], A. Kumar[63], E. Kun[11], N. Kurahashi[49], N. Lad[63], C. Lagunas Gualda[63], M. Lamoureux[37], M. J. Larson[19], S. Latseva[1], F. Lauber[62], J. P. Lazar[14, 40], J. W. Lee[56], K. Leonard DeHolton[60], A. Leszczyńska[44], M. Lincetto[11], Q. R. Liu[40], M. Liubarska[25], E. Lohfink[41], C. Love[49], C. J. Lozano Mariscal[43], L. Lu[40], F. Lucarelli[28], W. Luszczak[20, 21], Y. Lyu[8, 9], J. Madsen[40], K. B. M. Mahn[24], Y. Makino[40], E. Manao[27], S. Mancina[40, 48], W. Marie Sainte[40], I. C. Mariş[12], S. Marka[46], Z. Marka[46], M. Marsee[58], I. Martinez-Soler[14], R. Maruyama[45], F. Mayhew[24], T. McElroy[25], F. McNally[38], J. V. Mead[22], K. Meagher[40], S. Mechbal[63], A. Medina[21], M. Meier[16], Y. Merckx[13], L. Merten[11], J. Micallef[24], J. Mitchell[7], T. Montaruli[28], R. W. Moore[25], Y. Morii[16], R. Morse[40], M. Moulai[40], T. Mukherjee[31], R. Naab[63], R. Nagai[16], M. Nakos[40], U. Naumann[62], J. Necker[63], A. Negi[4], M. Neumann[43], H. Niederhausen[24], M. U. Nisa[24], A. Noell[1], A. Novikov[44], S. C. Nowicki[24], A. Obertacke Pollmann[16], V. O'Dell[40], M. Oehler[31], B. Oeyen[29], A. Olivas[19], R. Ørsøe[27], J. Osborn[40], E. O'Sullivan[61], H. Pandya[44], N. Park[33], G. K. Parker[4], E. N. Paudel[44], L. Paul[42, 50], C. Pérez de los Heros[61], J. Peterson[40], S. Philippen[1], A. Pizzuto[40], M. Plum[50], A. Pontén[61], Y. Popovych[41], M. Prado Rodriguez[40], B. Pries[24], R. Procter-Murphy[19], G. T. Przybylski[9], C. Raab[37], J. Rack-Helleis[41], K. Rawlins[3], Z. Rechav[40], A. Rehman[44], P. Reichherzer[11], G. Renzi[12], E. Resconi[27], S. Reusch[63], W. Rhode[23], B. Riedel[40], A. Rifaie[1], E. J. Roberts[2], S. Robertson[8, 9], S. Rodan[56], G. Roellinghoff[56], M. Rongen[26], C. Rott[53, 56], T. Ruhe[23], L. Ruohan[27], D. Ryckbosch[29], I. Safa[14, 40], J. Saffer[32], D. Salazar-Gallegos[24], P. Sampathkumar[31], S. E. Sanchez Herrera[24], A. Sandrock[62], M. Santander[58], S. Sarkar[25], S. Sarkar[47], J. Savelberg[1], P. Savina[40], M. Schaufel[1], H. Schieler[31], S. Schindler[26], L. Schlickmann[1], B. Schlüter[43], F. Schlüter[12], N. Schmeisser[62], T. Schmidt[19], J. Schneider[26], F. G. Schröder[31, 44], L. Schumacher[26], G. Schwefer[1], S. Sclafani[19], D. Seckel[44], M. Seikh[36], S. Seunarine[51], R. Shah[49], A. Sharma[61], S. Shefali[32], N. Shimizu[16], M. Silva[40], B. Skrzypek[14], B. Smithers[4], R. Snihur[40], J. Soedingrekso[23], A. Søgaard[22], D. Soldin[32], P. Soldin[1], G. Sommani[11], C. Spannfellner[27], G. M. Spiczak[51], C. Spiering[63], M. Stamatikos[21], T. Stanev[44], T. Stezelberger[9], T. Stürwald[62], T. Stuttard[22], G. W. Sullivan[19], I. Taboada[6], S. Ter-Antonyan[7], M. Thiesmeyer[1], W. G. Thompson[14], J. Thwaites[40], S. Tilav[44], K. Tollefson[24], C. Tönnis[56], S. Toscano[12], D. Tosi[40], A. Trettin[63], C. F. Tung[6], R. Turcotte[31], J. P. Twagirayezu[24], B. Ty[40], M. A. Unland Elorrieta[43], A. K. Upadhyay[40, 64], K. Upshaw[7], N. Valtonen-Mattila[61], J. Vandenbroucke[40], N. van Eijndhoven[13], D. Vannerom[15], J. van Santen[63], J. Vara[43], J. Veitch-Michaelis[40], M. Venugopal[31], M. Vereecken[37], S. Verpoest[44], D. Veske[46], A. Vijai[19], C. Walck[54], C. Weaver[24], P. Weigel[15], A. Weindl[31], J. Weldert[60], C. Wendt[40], J. Werthebach[23], M. Weyrauch[31], N. Whitehorn[24], C. H. Wiebusch[1], N. Willey[24], D. R. Williams[58], L. Witthaus[23], A. Wolf[1], M. Wolf[27], G. Wrede[26], X. W. Xu[7], J. P. Yanez[25], E. Yildizci[40], S. Yoshida[16], R. Young[36], F. Yu[14], S. Yu[24], T. Yuan[40], Z. Zhang[55], P. Zhelnin[14], M. Zimmerman[40]

[1] III. Physikalisches Institut, RWTH Aachen University, D-52056 Aachen, Germany
[2] Department of Physics, University of Adelaide, Adelaide, 5005, Australia
[3] Dept. of Physics and Astronomy, University of Alaska Anchorage, 3211 Providence Dr., Anchorage, AK 99508, USA
[4] Dept. of Physics, University of Texas at Arlington, 502 Yates St., Science Hall Rm 108, Box 19059, Arlington, TX 76019, USA
[5] CTSPS, Clark-Atlanta University, Atlanta, GA 30314, USA
[6] School of Physics and Center for Relativistic Astrophysics, Georgia Institute of Technology, Atlanta, GA 30332, USA
[7] Dept. of Physics, Southern University, Baton Rouge, LA 70813, USA
[8] Dept. of Physics, University of California, Berkeley, CA 94720, USA
[9] Lawrence Berkeley National Laboratory, Berkeley, CA 94720, USA
[10] Institut für Physik, Humboldt-Universität zu Berlin, D-12489 Berlin, Germany
[11] Fakultät für Physik & Astronomie, Ruhr-Universität Bochum, D-44780 Bochum, Germany
[12] Université Libre de Bruxelles, Science Faculty CP230, B-1050 Brussels, Belgium

[13] Vrije Universiteit Brussel (VUB), Dienst ELEM, B-1050 Brussels, Belgium

[14] Department of Physics and Laboratory for Particle Physics and Cosmology, Harvard University, Cambridge, MA 02138, USA

[15] Dept. of Physics, Massachusetts Institute of Technology, Cambridge, MA 02139, USA

[16] Dept. of Physics and The International Center for Hadron Astrophysics, Chiba University, Chiba 263-8522, Japan

[17] Department of Physics, Loyola University Chicago, Chicago, IL 60660, USA

[18] Dept. of Physics and Astronomy, University of Canterbury, Private Bag 4800, Christchurch, New Zealand

[19] Dept. of Physics, University of Maryland, College Park, MD 20742, USA

[20] Dept. of Astronomy, Ohio State University, Columbus, OH 43210, USA

[21] Dept. of Physics and Center for Cosmology and Astro-Particle Physics, Ohio State University, Columbus, OH 43210, USA

[22] Niels Bohr Institute, University of Copenhagen, DK-2100 Copenhagen, Denmark

[23] Dept. of Physics, TU Dortmund University, D-44221 Dortmund, Germany

[24] Dept. of Physics and Astronomy, Michigan State University, East Lansing, MI 48824, USA

[25] Dept. of Physics, University of Alberta, Edmonton, Alberta, Canada T6G 2E1

[26] Erlangen Centre for Astroparticle Physics, Friedrich-Alexander-Universität Erlangen-Nürnberg, D-91058 Erlangen, Germany

[27] Technical University of Munich, TUM School of Natural Sciences, Department of Physics, D-85748 Garching bei München, Germany

[28] Département de physique nucléaire et corpusculaire, Université de Genève, CH-1211 Genève, Switzerland

[29] Dept. of Physics and Astronomy, University of Gent, B-9000 Gent, Belgium

[30] Dept. of Physics and Astronomy, University of California, Irvine, CA 92697, USA

[31] Karlsruhe Institute of Technology, Institute for Astroparticle Physics, D-76021 Karlsruhe, Germany

[32] Karlsruhe Institute of Technology, Institute of Experimental Particle Physics, D-76021 Karlsruhe, Germany

[33] Dept. of Physics, Engineering Physics, and Astronomy, Queen's University, Kingston, ON K7L 3N6, Canada

[34] Department of Physics & Astronomy, University of Nevada, Las Vegas, NV, 89154, USA

[35] Nevada Center for Astrophysics, University of Nevada, Las Vegas, NV 89154, USA

[36] Dept. of Physics and Astronomy, University of Kansas, Lawrence, KS 66045, USA

[37] Centre for Cosmology, Particle Physics and Phenomenology - CP3, Université catholique de Louvain, Louvain-la-Neuve, Belgium

[38] Department of Physics, Mercer University, Macon, GA 31207-0001, USA

[39] Dept. of Astronomy, University of Wisconsin–Madison, Madison, WI 53706, USA

[40] Dept. of Physics and Wisconsin IceCube Particle Astrophysics Center, University of Wisconsin–Madison, Madison, WI 53706, USA

[41] Institute of Physics, University of Mainz, Staudinger Weg 7, D-55099 Mainz, Germany

[42] Department of Physics, Marquette University, Milwaukee, WI, 53201, USA

[43] Institut für Kernphysik, Westfälische Wilhelms-Universität Münster, D-48149 Münster, Germany

[44] Bartol Research Institute and Dept. of Physics and Astronomy, University of Delaware, Newark, DE 19716, USA

[45] Dept. of Physics, Yale University, New Haven, CT 06520, USA

[46] Columbia Astrophysics and Nevis Laboratories, Columbia University, New York, NY 10027, USA

[47] Dept. of Physics, University of Oxford, Parks Road, Oxford OX1 3PU, United Kingdom

[48] Dipartimento di Fisica e Astronomia Galileo Galilei, Università Degli Studi di Padova, 35122 Padova PD, Italy

[49] Dept. of Physics, Drexel University, 3141 Chestnut Street, Philadelphia, PA 19104, USA

[50] Physics Department, South Dakota School of Mines and Technology, Rapid City, SD 57701, USA

[51] Dept. of Physics, University of Wisconsin, River Falls, WI 54022, USA

[52] Dept. of Physics and Astronomy, University of Rochester, Rochester, NY 14627, USA

[53] Department of Physics and Astronomy, University of Utah, Salt Lake City, UT 84112, USA

[54] Oskar Klein Centre and Dept. of Physics, Stockholm University, SE-10691 Stockholm, Sweden

[55] Dept. of Physics and Astronomy, Stony Brook University, Stony Brook, NY 11794-3800, USA

[56] Dept. of Physics, Sungkyunkwan University, Suwon 16419, Korea

[57] Institute of Physics, Academia Sinica, Taipei, 11529, Taiwan

[58] Dept. of Physics and Astronomy, University of Alabama, Tuscaloosa, AL 35487, USA

[59] Dept. of Astronomy and Astrophysics, Pennsylvania State University, University Park, PA 16802, USA

[60] Dept. of Physics, Pennsylvania State University, University Park, PA 16802, USA

[61] Dept. of Physics and Astronomy, Uppsala University, Box 516, S-75120 Uppsala, Sweden

[62] Dept. of Physics, University of Wuppertal, D-42119 Wuppertal, Germany

[63] Deutsches Elektronen-Synchrotron DESY, Platanenallee 6, 15738 Zeuthen, Germany

[64] Institute of Physics, Sachivalaya Marg, Sainik School Post, Bhubaneswar 751005, India

[65] Department of Space, Earth and Environment, Chalmers University of Technology, 412 96 Gothenburg, Sweden

[66] Earthquake Research Institute, University of Tokyo, Bunkyo, Tokyo 113-0032, Japan

Acknowledgements

PoS(ICRC2023)1046